J Mol Model (2015) 21:149
DOI 10.1007/s00894-015-2684-3

ORIGINAL PAPER

# Molecular simulations of mixed self-assembled monolayer coated gold nanoparticles in water

**Meena Devi J** [1]

Received: 28 October 2014 / Accepted: 27 April 2015


**Abstract** Molecular dynamics simulations have been employed to study the hydration of a series of nanoparticles, each of which was coated with a mixed self-assembled monolayer (SAM) comprising methyl- and hydroxy-terminated alkane thiol chains. The mixing ratio of those chains are different for each nanoparticle. The simulations focused on the wetting behavior of the SAM-coated gold nanoparticles and the distribution and structure of their interfacial water molecules. The interactions of the mixed SAM-coated gold nanoparticles with water were analyzed by evaluating the radial distribution function, hydrogen bonds, the dipole orientations of the water molecules, and the water residence time in the interfacial region. The wettability of the mixed SAM-coated gold nanoparticles improved as the concentration of terminal hydroxy moieties was increased. The distribution and dynamics of the interfacial water molecules were found to be influenced by the mixing ratio of the terminal moieties of the SAM chains. The results of our simulations suggest that the surface interactions of the mixed SAM-coated gold nanoparticles with the aqueous medium can be modulated by systematically altering the mixing ratio of the terminal methyl and hydroxy moieties. This work may lead to new biological and technological applications and inspire the development of novel biomimetic materials.

**Keywords** Gold nanoparticles · Mixed SAM · Alkane thiol · Hydration · Molecular dynamics simulation

✉ Meena Devi J
jmeenadevi@sastra.ac.in

[1] Centre for Nanotechnology & Advanced Biomaterials (CeNTAB) and School of Electrical & Electronics Engineering (SEEE), SASTRA University, Thanjavur 613401, Tamilnadu, India

## Introduction

Gold nanoparticles have been studied extensively due to their unique size-dependent physical and chemical properties, biocompatibility, and potential applications in a wide range of fields, such as optics, electronics, sensors, chemistry, biology, medicine, engineering, and technology [1–4]. Generally, gold nanoparticles are protected by coating them with a self-assembled monolayer (SAM) of organic molecules to improve their stability and enrich their functional diversity [5, 6]. The functional groups of the protecting monolayer can modify, control, and regulate the properties and surface interactions of the gold nanoparticles. The special features of SAM-coated gold nanoparticles make them suitable for a broad range of applications, such as molecular electronics, protective coatings, wetting, adhesion, drug carriers, therapeutic agents, sensors, molecular recognition, diagnostic tools, cell attachment, biomaterials, biological interfaces, biological probes, and so on [7–12].

SAMs comprising more than one type of passivating ligand molecule are called mixed SAMs. A mixed self-assembled monolayer is composed of a combination of polymers with either different surface functional groups or different chain lengths. Mixed ligand gold nanoparticles have been found to adopt several kinds of ligand shell organization including Janus-type, striped patterns, and random dispersion at the nanoparticle surface [13–18]. The ability of mixed SAMs to control and alter the interfacial properties of gold could be harnessed in applications such as biosensors, targeted drug delivery, molecular recognition, protein adsorption, and the immobilization of macromolecules [19–25]. Computer simulations are emerging as a powerful technique for understanding and solving the challenges and issues associated with the fields of materials science, biology, and engineering. Simulation studies of nanoscale materials can enrich our understanding of

Published online: 20 May 2015

their structures, driving forces, interactions, and properties, and can provide insights into the structure–property relationship at the atomic and molecular levels. In the literature, some molecular simulation studies of mixed SAMs on gold surfaces and gold nanoparticles have been reported, centering on their structures and their interactions with water and proteins [26–31].

The motivation for the study of a chemically heterogeneous system such as mixed SAM-coated gold nanoparticles stems from the functioning and salient properties of the molecules in a biological system, which consists of about 70 % water. The amazing natural functions of biological molecules arise through their complex chemical compositions (combinations of hydrophobic and hydrophilic regions), intricate structures, dynamics, and their chemical and physical interactions with water and other interlinked biological components. The surfaces of mixed SAM-coated gold nanoparticles partly mimic biological molecules; therefore, in the long run, mixed SAM-coated gold nanoparticles may be utilized in the development of smart machines or to build artificial lifeforms (e.g., advanced robots) that incorporate advances in the field of artificial intelligence.

Mixed SAM systems can serve as simple model systems to study the fundamental aspects of interfacial water and to investigate the interactions of complex bioinorganic nanostructures such as proteins, antibodies, and the membrane properties of cells [8]. The interactions of mixed SAM systems with water directly impact processes such as protein folding, membrane formation, and colloidal and biological self-assembly. A characteristic feature of mixed SAMs is the ability to easily modify their chemical compositions experimentally in a deliberate manner. Gold nanoparticles protected by mixed SAMs with both hydrophobic and hydrophilic terminal groups are very useful for biological applications. A good understanding and systematic control of the interactions of mixed SAM-coated gold nanoparticles with an aqueous medium will aid the fabrication of functionalized gold nanoparticles for biological applications such as biomolecular recognition, protective coatings, biomaterials, biological interfaces, and biosensors.

Ultrasmall gold nanoparticles with core diameters of around 0.8 nm and short alkane thiol chains were studied in the work reported in the present paper. Such ultrasmall gold nanoparticles with core diameters of<3 nm may be advantageous for some biological and technological applications in which the gold nanoparticles are placed in a small target region in order to achieve selective and enhanced interactions as well as better performance [32–34]. Moreover, ultrasmall gold nanoparticles have been found to exhibit interesting magnetic, optical, redox, and catalytic properties [35–38]. Properties such as the conformational order, friction, wettability, and distance control depend on the length of the alkane thiol chains. Short alkane thiol chains have been found to exhibit high friction and lower hydrophobicity, and they promote smaller interparticle spacing during self-assembly as well as a shorter distance between the guest and target molecule [39–43]. Hence, in applications that demand the above features, ultrasmall gold nanoparticles with short thiol chains can enhance performance (in terms of sensing, binding, detection, and so on).

In the present study, five mixed SAM-coated gold nanoparticles with different ratios of methyl-terminated (hydrophobic) to hydroxy-terminated (hydrophilic) alkane thiol chains in water solvent were simulated to explore and examine their wetting behavior, the distribution and dynamics of their interfacial water, and the effect of the mixing ratio of the terminal moieties. The results of this computational study allow a greater molecular level understanding of the interaction of mixed SAM-coated gold nanoparticles with surrounding water molecules, as well as the microscopic distribution of the interfacial water molecules. The outcome of this work may aid the surface engineering of monolayer-protected gold nanoparticles and inspire the development of novel biomimetic materials and devices.

## Materials and methods

Five mixed SAM-coated gold nanoparticle systems were constructed with different ratios (1:0, 2:1, 1:1, 1:2, 0:1) of methyl-terminated to hydroxy-terminated alkane thiol chains; these were labeled systems A, B, C, D, and E, respectively. The different SAM compositions of these five systems are illustrated schematically in Fig. 1. Each system comprised a single mixed SAM-coated gold nanoparticle solvated in a water box. The protecting monolayer had a chemical composition of S–$[CH_2]_6$–X, where X is the terminal group (either a methyl or a hydroxy group). The united atom model was applied to the methylene and methyl groups. The size of a bare gold

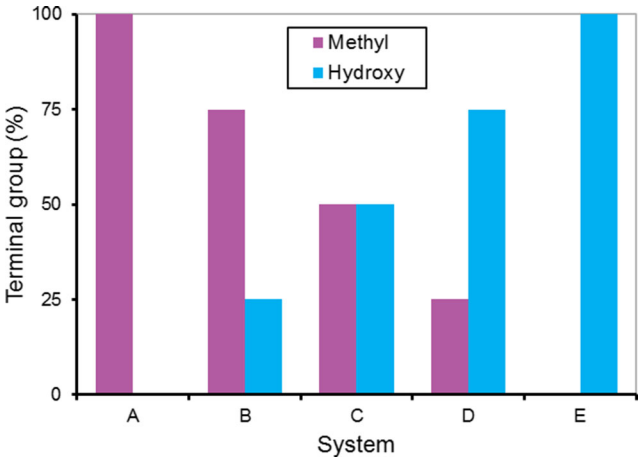


**Fig. 1** Schematic representation illustrating the differences in composition among the five mixed SAM-coated gold nanoparticle systems

nanoparticle calculated using the radius of gyration was 7.8 Å, and it contained 249 atoms. The alkane thiol chains are set in a *trans* configuration with their sulfur head groups perpendicular to the gold surface and attached in the atop position. A random morphology of the mixed monolayer was assumed, as experimentally ordered domains have been observed for gold nanoparticles with core diameters ranging from 25 to 80 Å [15, 16]. The mixed SAMs were generated by randomly placing methyl- and hydroxy-terminated alkane thiol chains on the surface of the gold core.

The force-field parameters for the gold and the alkane thiol chains were obtained from the literature [44–46] and used in the present work without any modifications. They are described in detail in our previous report [47]. The model and force-field parameters used here were validated in our previous work on thiol-coated gold nanoparticles [47]. Moreover, significant results of employing these force-field parameters for gold systems have been reported in the literature [48, 49]. All of the molecular dynamics simulations were performed with the NAMD2.9 package [50]. The systems were simulated under the isobaric–isothermal (NPT) ensemble. The TIP3P water model [51] was used and pressure was held at a constant value of 1.013125 bar. Langevin dynamics was used with a damping coefficient of 5/ps for temperature control. Periodic boundary conditions were imposed, corresponding to a box of dimensions 57×60× 58 $Å^3$. The particle mesh Ewald method was employed for long-range electrostatics. Energy minimizations were performed using conjugate gradient energy minimization, and the number of steps performed during minimization was 3000. A time step of 2 fs was used when integrating the equations of motion, and all of the systems were run for 20 ns at room temperature. All of the analysis focused on the last 5 ns of the simulation. The water molecules within 4 Å of the mixed SAM-coated gold nanoparticles were considered the interfacial water molecules.

## Results and discussion

Molecular dynamics simulations of the mixed SAM-coated gold nanoparticles in water solvent were carried out for a period of 20 ns at room temperature. All five systems reached a stable state during the simulated time period of 20 ns. As an example, the total energy of a mixed SAM-coated gold nanoparticle corresponding to system B as a function of time is given in Fig. 2. Snapshots of the monolayer-protected gold nanoparticles at the end of the simulations are displayed in Fig. 3. Quantitative differences in the sizes of these systems were demonstrated by analyzing their radii of gyration, as presented in Fig. 4 and Table 1. There are minor but distinct differences (of <1 Å) in the sizes of the mixed SAM-coated gold nanoparticles. Within this small range of sizes, there is a gradual increase in the average size of the system with

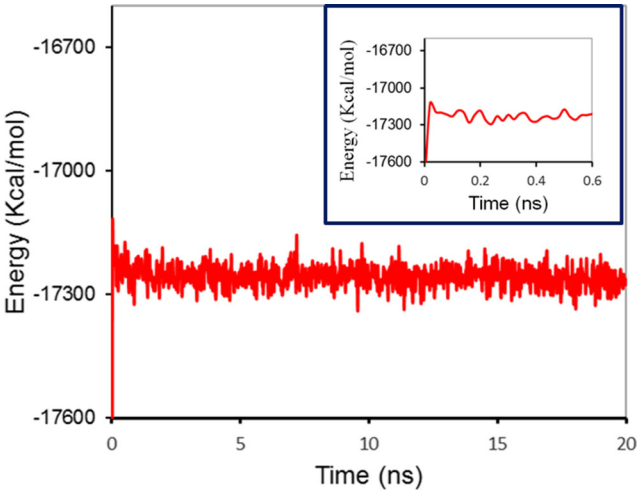


**Fig. 2** Total energy of a mixed SAM-coated gold nanoparticle (system B)

increasing concentration of the terminal hydroxy moiety. This may be due to the affinity of hydroxy groups for water molecules, meaning that the hydroxy chains stretch and spread themselves to allow water molecules to get closer to them. Lehn and Alexander-Katz [31] investigated the three morphological types of mixed-ligand gold nanoparticles in aqueous solution using molecular dynamics simulation. They showed that hydrophobic alkane thiol ligand chains were able to bend more to avoid exposure to solvent molecules while ensuring that the hydroxy terminal groups were always exposed to water [31].

### Distribution of water molecules

The distribution of the interfacial water molecules can be assessed by calculating the average number of water molecules at the interface between them and the mixed SAM-coated gold nanoparticle. The time-averaged total number of interfacial water molecules for each mixed SAM-coated gold nanoparticle is depicted in Fig. 5 and Table 1. Among the five simulated systems, the average number of water molecules that reside in the interfacial region is smallest for the hydrophobic homoligand gold nanoparticle, largest for the hydrophilic homoligand gold nanoparticle, and intermediate for the mixed ligand gold nanoparticles. This reveals that the mixed ligand gold nanoparticles show partial wetting behavior. Due to the mixed surface chemistry, the number of interfacial water molecules for each mixed ligand gold nanoparticle lies between the corresponding numbers for the homoligand methyl-terminated and hydroxy-terminated gold nanoparticles. The wettability of the mixed ligand gold nanoparticle varies with the mixing ratio of the terminal moieties. In the literature, similar simulation and experimental results have been reported for mixed alkane thiol surfaces [26, 52, 53]. Increasing the concentration of terminal hydroxy moieties

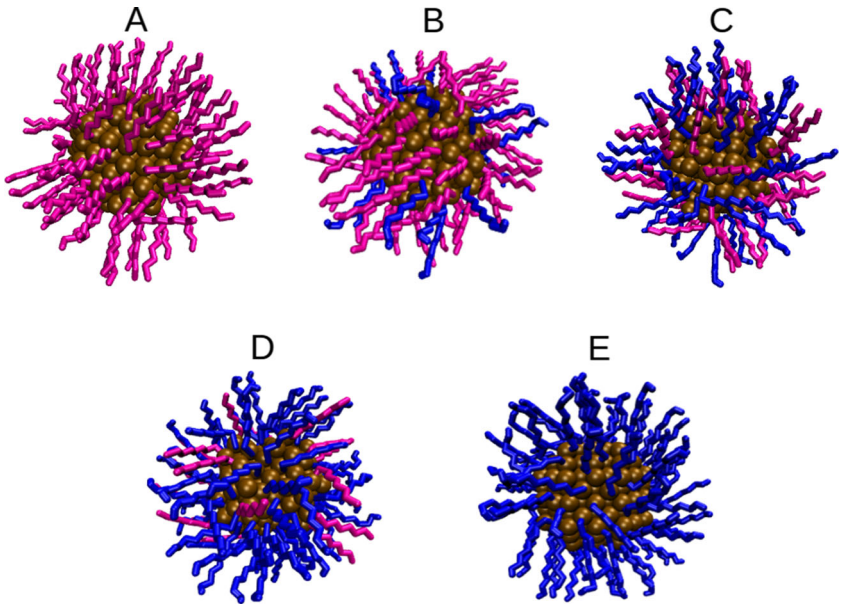


**Fig. 3** Snapshots of the mixed SAM-coated gold nanoparticles at the end of the simulation. Gold atoms (*brown*) are given in *van der Waals representation*. Methyl-terminated (*pink*) and hydroxy-terminated (*blue*) alkane thiol chains are given in *licorice representation*. Water molecules are not shown for the sake of clarity

leads to increased wetting, which may be attributed to the enhanced hydrophilic interactions between the mixed SAM surface and the proximate water molecules.

The structural organization and the spatial distribution of the water molecules at the interface with each mixed SAM-coated gold nanoparticle can be obtained from the radial distribution function (RDF) between the terminal groups of the SAM chains and the water molecules (Fig. 6). The water molecules are highly structured with respect to the terminal groups, as shown in Fig. 6, and this influences their dynamics. A molecular dynamics simulation study reported in the literature indicated that there is a well-defined hydration layer at the interface with the homoligand gold nanoparticle [54]. The observed differences between the structure of the first hydration shell of each mixed ligand gold nanoparticle and the structure of the first hydration shell for either the hydrophobic or hydrophilic homoligand gold nanoparticle indicate that the mixed ligand gold nanoparticles show different wetting behavior from the homoligand gold nanoparticles. The position of the first peak in the RDF (corresponding to the position of the first hydration shell) is similar for all of the mixed ligand gold nanoparticles and the hydroxy homoligand gold nanoparticle, but the peak heights differ. The degree of hydrophilicity of the mixed SAM surface can affect the peak height in the radial distribution function.

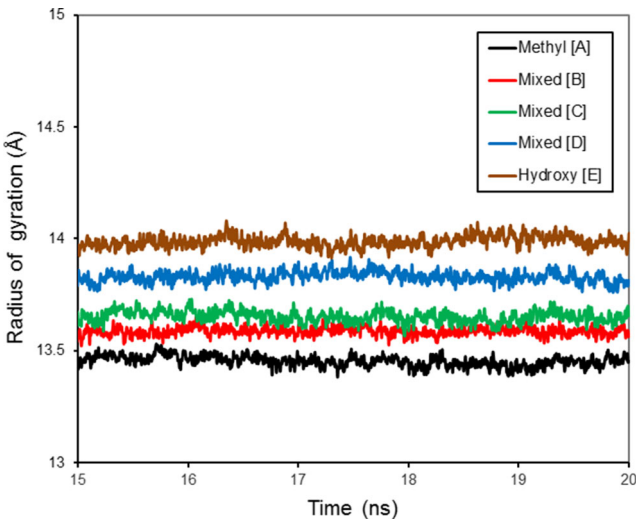


**Fig. 4** Radii of gyration of the mixed SAM-coated gold nanoparticles

In Fig. 6, the peaks occur at about 2.6 Å, corresponding to the nearest-neighbor distance between the polar hydroxy groups and the water oxygen atoms. These peaks originate from the strong interactions between the hydrophilic terminal groups and the vicinal water molecules via hydrogen bonds. The probability that a water molecule will be found in the first hydration shell of the mixed ligand gold nanoparticle increases with the concentration of hydroxy-terminated SAM chains. This is consistent with the result inferred from Fig. 5. The attractive interactions between the hydrophilic terminal groups and the surrounding water molecules can enhance the concentration of bound water molecules at the interface. The position of the first RDF peak (i.e., the first hydration shell) for the hydrophobic homoligand gold nanoparticle shifts to 3.7 Å, as the hydrophobic methyl groups do not allow the oxygen atoms of the water molecules to get very close to them [28]. This reduces the penetration of water molecules into the interfacial region of the methyl-terminated gold nanoparticle.

The interfacial water of the mixed SAM-coated gold nanoparticles shows different behavior from bulk water. The water–water pair correlation function is sensitive to the surface chemistry. The pair correlation functions of the interfacial

**Table 1** Sizes of the mixed SAM-coated gold nanoparticles and the average number of water molecules at the interface with each SAM-coated gold nanoparticle

| System | Mixing ratio of terminal groups (methyl:hydroxy) | Average size (Å) | Average number of interfacial water molecules |
|---|---|---|---|
| A | 1:0 | 13.49±0.02 | 164±14 |
| B | 2:1 | 13.59±0.02 | 341±14 |
| C | 1:1 | 13.65±0.03 | 426±13 |
| D | 1:2 | 13.81±0.03 | 476±13 |
| E | 0:1 | 14.00±0.03 | 520±13 |

water oxygen atoms of the mixed SAM-coated gold nanoparticles along with the corresponding function for the bulk water are shown in Fig. 7. In bulk water, the first peak at 2.8 Å corresponds to nearest-neighbor hydrogen bonding. For the interfacial water of the monolayer-protected gold nanoparticles, the location of the first peak remains the same but its height is enhanced. This may be due to enhanced short-range correlations.

## Hydrogen bonds

The structural organization and the dynamics of the interfacial water molecules are dependent on the network of hydrogen bonds present. The hydrogen-bond structure of water plays an important role in physical, chemical, and biological processes. The hydrogen-bond interactions between the mixed SAM surface and the water molecules may play a role in the development of biosensors and biological interfaces. The hydrogen-bonding network of the interfacial water of mixed SAM-coated gold nanoparticles can be assessed by calculating the average number of hydrogen bonds between the terminal groups of the SAM chains and the surrounding water molecules. The geometric criteria adopted for this hydrogen-bond calculation in our work were a cutoff angle of 30° for the donor–hydrogen–acceptor angle and a cutoff distance of 3.6 Å for the donor–acceptor distance. The total number of hydrogen bonds between the terminal group of a SAM chain and the water molecules for each of the five simulated systems is presented in Fig. 8. As expected, there was no hydrogen-bond formation between the water solvent and the terminal groups of the hydrophobic homoligand gold nanoparticle.

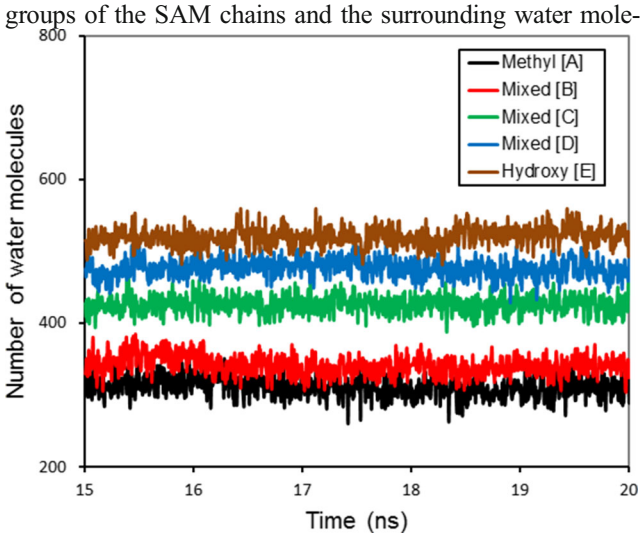


**Fig. 5** Total number of water molecules in the interfacial region of each mixed SAM-coated gold nanoparticle

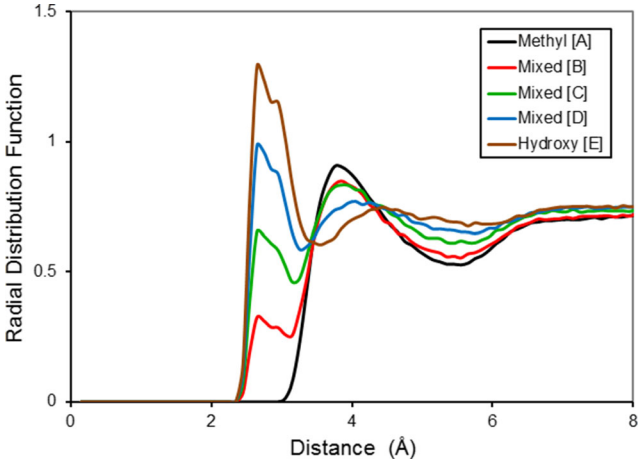


**Fig. 6** Radial distribution functions between the terminal groups of the mixed SAM-coated gold nanoparticles and the oxygen atoms of surrounding water molecules

There are intermolecular hydrogen bonds in addition to the intramolecular hydrogen bonds between the water molecules in the vicinal water of the hydrophilic homoligand gold nanoparticle and mixed ligand gold nanoparticles. The hydrogen-bond network of interfacial water is therefore more disrupted than the extended hydrogen-bond network of the bulk water. The average number of interfacial hydrogen bonds increases with increasing concentration of hydrophilic terminal groups. Zheng et al. [28] have reported that the total number of interfacial hydrogen bonds with hydroxy-terminated alkane thiol chains increases as the concentration of such chains increases, according to their molecular simulation study of a mixed SAM gold surface.

The difference observed in the number of interfacial hydrogen bonds means that a relatively larger number of water molecules are retained near to the hydrophilic gold nanoparticle and a moderately large population of water molecules are retained near each mixed ligand gold nanoparticle as compared to the number of water molecules retained close to the hydrophobic homoligand gold nanoparticle (Table 1, Fig. 5). The number of interfacial hydrogen bonds is thus dependent on the mixing ratio of the terminal moieties. This suggests that hydrogen-bond interactions between the molecular surface of the gold nanoparticle and any target molecule or aqueous medium of interest could be controlled by varying the mixing ratio of the terminal functional groups of the SAM chains.

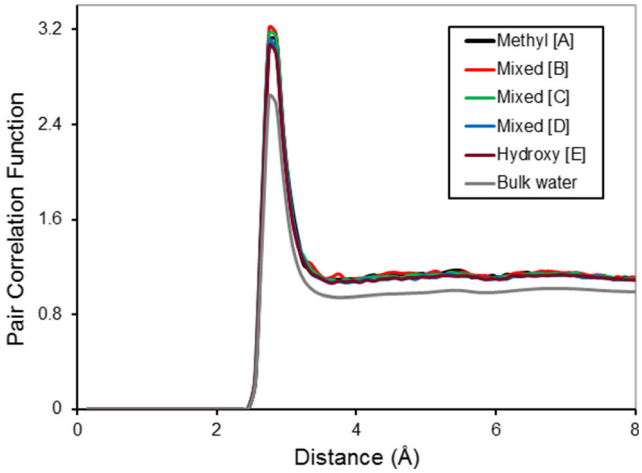


**Fig. 7** Pair correlation functions between the water molecules in the interfacial regions of the mixed SAM-coated gold nanoparticles

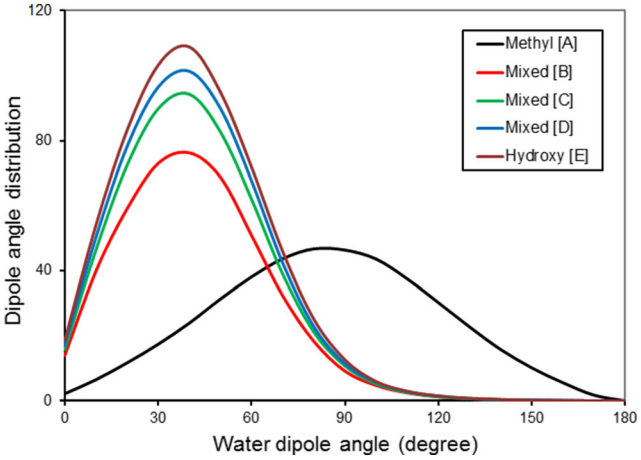


**Fig. 9** Orientations of water dipole vectors in the interfacial regions of mixed SAM-coated gold nanoparticles

## Orientation of water molecules

The orientation of the water molecules at the interface can influence the processes of molecular recognition, molecular orientation, and self-assembly. To elucidate the ordering and orientation of the water molecules in the interfacial region with each mixed SAM-coated gold nanoparticle, the distribution of water dipole angles was determined, and this is displayed in Fig. 9. The water dipole angle is defined as the angle between the vector of the dipole of water and the vector connecting the oxygen atom of a water molecule with the center of mass of the nanoparticle. The distribution of water dipole angles is flat for bulk water since all orientations of water molecules are equally probable. The orientation of the water molecules is strongly related to the interaction force. The preferred orientation of the water molecules in the interfacial region can be discerned from the position of each peak in Fig. 9. Experimental measurements have revealed the ordering of water molecules at the interface between phospholipid monolayers and a hydrophobic surface [55, 56]. Heikkila et al. [57] investigated charged monolayer-protected gold nanoparticles in aqueous solution by performing molecular dynamics simulations. They reported the preferred orientations of the water molecules in the interfacial regions of alkane thiol capped gold nanoparticles.

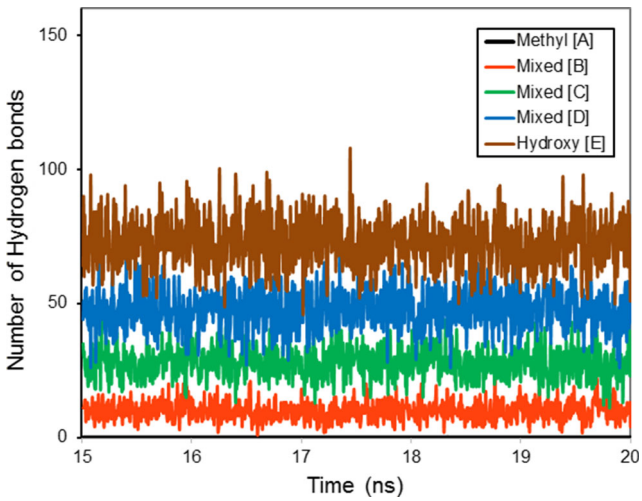


**Fig. 8** Total number of hydrogen bonds between the terminal group of a SAM chain and the water molecules for each of the five simulated systems A–E

The homoligand and mixed ligand gold nanoparticles induce significant reorientation of the water molecules at the interface. In the case of the hydrophobic homoligand gold nanoparticle, there is a single smooth and broad peak with a center at 90° (Fig. 9). This preferred orientation of the water molecules minimizes the interaction between the water molecules and the hydrophobic surface. The mixed ligand gold nanoparticles show the same orientational preference of vicinal water molecules in the interfacial region as seen for the homoligand hydrophilic gold nanoparticle. For all of these nanoparticles, the water dipole angle distribution is relatively narrow, and the most probable angle is 40°. This narrow distribution can be attributed to the biased orientation of the water molecules towards the hydroxy terminal groups, and the hydrogen bonds that they form with those groups. However, the height of the peak in the distribution increases with increasing concentration of hydroxy terminal groups. This increase in peak height occurs because the overall hydrophilicity of the mixed SAM surface rises as the concentration of hydroxy terminal moieties increases [58].

The observed trend in the orientation of the water molecules also implies that introducing hydrophilic terminal groups into a coating with only hydrophobic terminal groups elevates the hydrophilicity and suppresses the hydrophobicity of the surface to some extent, even when the hydrophilic terminal groups are only present at low concentrations. The magnitude of the dipole angle distribution increases with increasing concentration of hydrophilic terminal groups on the mixed

SAM-coated gold nanoparticle as the hydrophilic interaction with the surface strengthens. The structure and conformation of the water molecules in the interfacial region play a role in the adsorption of ions and proteins at the surface. This may therefore open up the possibility of controlling the interactions between target molecules and mixed ligand gold nanoparticles by varying the mixing ratio of the terminal methyl and hydroxy functional groups of the SAM chains.

## Residence time of water molecules

The dynamics of water is influenced by environmental conditions and by the physical and chemical properties of any solutes present. The dynamics of water around the mixed SAM gold nanoparticles could play a role in the biological activities of those systems. The mobility of the water molecules in the interfacial region can be quantitatively determined via the residence time, which can in turn be obtained from the residence time correlation function $R(t)$. This function is defined in terms of the Heaviside step function ($p_i$), and can be expressed as

$$R(t) = \left\langle \frac{1}{N} \sum_{i=1}^{N} p_i(t_0) p_i(t_0 + t) \right\rangle, \quad (1)$$

where $N$ is the number of water molecules residing within the selected water layer. In Eq. 1, the Heaviside function takes a value of 1 when a water molecule is present in the selected region in the period $t_0$ to $t$ and a value of 0 otherwise. The computed residence-time correlation functions for the interfacial water molecules with systems A–E are plotted in Fig. 10. The relaxation of $R(t)$ illustrates the local dynamics of the hydration water. In Fig. 10, the time evolution of the correlation function is biphasic: there is initially a fast decay, which later gives way to a slow decay. The residence-time correlation function can therefore be fitted by a double exponential function, and the values of the corresponding fitting parameters are given in Table 2.

$$R(t) = Xe^{\frac{-t}{\tau_s}} + Ye^{\frac{-t}{\tau_l}}$$

Here, $\tau_s$ and $\tau_l$ represent short and long residence time constants.

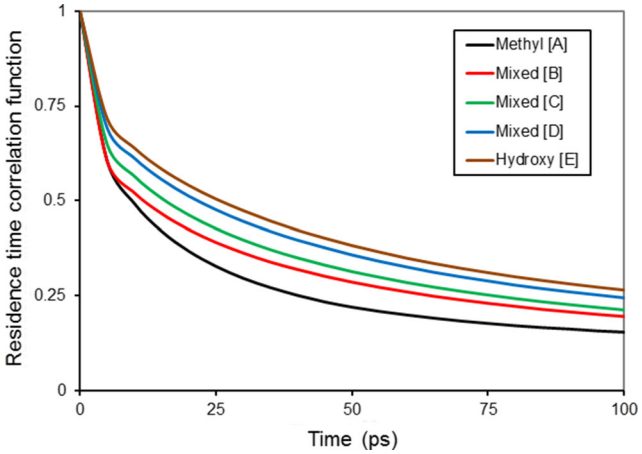


**Fig. 10** Residence-time correlation functions for the water molecules in the interfacial regions of the mixed SAM-coated gold nanoparticles

The timescale of motion of the water molecules drives the degree of order in the dynamics of the water molecules. The short residence-time constant corresponds to the water molecules that remain in the hydration shell only briefly, and relates to the spatially restricted librational (hindered rotation) and vibrational motion of the water molecules [59, 60]. The fast component of the water relaxation in the mixed SAM systems takes values ranging between 4.0 and 6.0 ps. The fast-vibrating mode can be viewed as the vibration of quasi-free water molecules in a temporary microscopic cage formed by their neighboring molecules. The long residence-time constant corresponds to water molecules that stay in the hydration shell for prolonged periods of time, and relates to rotational and translational motion of the water molecules [59, 60]. The residence-time correlation functions exhibit a slow component at long times (95–113 ps). The slow relaxation component signifies a restricted environment and reflects the dynamics of bound water molecules.

Integration of the residence-time correlation function yields the average residence time $\tau$:

$$\tau = \int_0^\infty R(t)dt$$

The calculated values of the residence time are reported in Table 2. The residence-time values calculated for the mixed ligand gold nanoparticle systems B, C, and D are 55.51, 62.23,

**Table 2** Fitting parameters for the time correlation function and the water residence time $\tau$

| Parameters | System A (methyl SAM) | System B (mixed SAM) | System C (mixed SAM) | System D (mixed SAM) | System E (hydroxy SAM) |
|---|---|---|---|---|---|
| $X$ | 0.49 | 0.45 | 0.39 | 0.37 | 0.35 |
| $Y$ | 0.51 | 0.55 | 0.60 | 0.63 | 0.64 |
| $\tau_s$ (ps) | 4.09 | 4.62 | 4.90 | 5.23 | 5.73 |
| $\tau_l$ (ps) | 95.17 | 97.14 | 103.33 | 108.17 | 112.75 |
| $\tau$ (ps) | 50.54 | 55.51 | 62.23 | 70.08 | 74.16 |

and 70.08 ps, respectively. The residence-time values calculated for the methyl- and hydroxy-terminated homoligand gold nanoparticles are 50.54 and 74.16 ps, respectively. The error involved in calculating the water-residence time is around 2 %. The residence time of interfacial water molecules is much longer than that of bulk water. Experimental studies have highlighted the slow dynamic behavior of interfacial water around a protein and a polymer [60, 61]. Li et al. [54] report that the residence time of interfacial water for a monolayer-protected gold nanoparticle is longer than that of bulk water. The long residence time of interfacial water indicates the presence of strong interactions between the alkane thiol SAM and the water molecules [62]. The residence time of the water molecules close to the hydrophilic surface region is longer than that of the water molecules close to the hydrophobic surface region. This result is consistent with results reported in the literature [63].

Generally, the water-residence time at the interface is found to be influenced by the chemical nature and topology of the system as well as the hydrogen bonds present. The residence-time values for the mixed SAM-coated nanoparticles lie in-between the values for the methyl- and hydroxy-terminated homoligand gold nanoparticles. This indicates that the adsorption of the vicinal water molecules influences both the terminal hydrophobic and the terminal hydrophilic moieties. The chemical heterogeneity of the surface modulates the residence time. The variability noted in the residence times obtained in the present simulations may reflect differences in the number of interfacial hydrogen bonds, the overall hydrophilicity, and the hydrating ability of the surface among the monolayer-protected gold nanoparticles. For the three mixed ligand gold nanoparticles, the residence time increased with the percentage of terminal hydroxy groups. Strengthening the surface hydrophilic interactions and creating a greater number of interfacial hydrogen bonds can constrain the mobility of the vicinal water molecules and slow down their dynamics. The spread and the linear variation found in the computed residence times for different mixing ratios of the terminal groups suggests the possibility of controlling the temporal behavior of interfacial water by adjusting the ratio of terminal surface functionalities.

## Conclusions

In this computational study, molecular dynamics simulations were performed to investigate the hydration of mixed SAM-coated gold nanoparticles consisting of binary mixtures of methyl- and hydroxy-terminated alkane thiol chains, emphasizing their wetting behavior and the structure of their interfacial water. The simulation results were discussed in terms of the spatial distribution of the water molecules, hydrogen bonds, water dipole orientations, and the water-residence time. The wettability of the mixed SAM-coated gold nanoparticles was found to be linearly related to the concentration of terminal hydroxy moieties. The mixed SAM-coated gold nanoparticles exerted strong influence on the structure and dynamics of the interfacial water. The structure of the interfacial water varied with changes in the concentrations of the terminal methyl and hydroxy moieties of the SAM chains. Hence, the interactions of mixed SAM-coated gold nanoparticles with an aqueous medium can be modified by adjusting the mixing ratio of the terminal methyl and hydroxy moieties. The results of the present work may be used to guide the experimental design of functionalized gold nanoparticles and to choose the appropriate mixing ratios of terminal moieties for specific biological and technological applications that are based on the hydrophobic and hydrophilic interactions of nanostructured materials in an aqueous medium. This work could be further extended by allowing the mixed SAM-coated gold nanoparticles to interact with other biomolecules or by varying the chemical composition of the SAM to include amino, phenyl, carboxyl group or peptide, DNA, and PEG groups. The length of the SAM chains can be varied depending on the study and application. Such a series of simulation studies could aid the design and development of functionalized gold nanoparticles for practical applications such as sensing, protective coating, biological interface, and diagnostic tool.

**Acknowledgments** The computing time at the Annapurna cluster, The Institute of Mathematical Sciences, Chennai, India is appreciated.

## References

1. Daniel M, Astruc D (2004) Gold nanoparticles: assembly, supramolecular chemistry, quantum-size-related properties, and applications toward biology, catalysis, and nanotechnology. Chem Rev 104:293–346. doi:10.1021/cr030698+
2. Arvizo RR, Bhattacharyya S, Kudgus RA, Giri K, Bhattacharya R, Mukherjee P (2012) Intrinsic therapeutic applications of noble metal nanoparticles: past, present and future. Chem Soc Rev 41:2943–2970. doi:10.1039/c2cs15355f
3. Ghosh SJ, Pal T (2007) Interparticles coupling effect on the surface plasmon resonance of gold nanoparticles: from theory to applications. Chem Rev 107:4797–4862. doi:10.1021/cr0680282
4. Wilson R (2008) The use of gold nanoparticles in diagnostics and detection. Chem Soc Rev 37:2028–2045. doi:10.1039/b712179m
5. Ofir Y, Bappaditya RVM (2008) Polymer and biopolymer mediated self-assembly of gold nanoparticles. Chem Soc Rev 37:1814–1825. doi:10.1039/B712689C
6. Whitesides GM, Kriebel JK, Love JC (2005) Molecular engineering of surfaces using self-assembled monolayers. Sci Prog 88:17–48. doi:10.3184/003685005783238462
7. Fendler JH (2001) Chemical self-assembly for electronic applications. Chem Mater 13:3196–3210. doi:10.1021/cm010165m
8. Love JC, Estroff LA, Kriebel JK, Nuzzo RG, Whitesides GM (2005) Self-assembled monolayers of thiolates on metals as a form of nanotechnology. Chem Rev 105:1103–1170. doi:10.1021/cr0300789

9. Dykman L, Khlebtsov N (2012) Gold nanoparticles in biomedical applications: recent advances, and perspectives. Chem Soc Rev 41: 2256–2282. doi:10.1039/C1CS15166E
10. Rana S, Bajaj A, Mout R, Rotello VM (2012) Monolayer coated gold nanoparticles for delivery applications. Adv Drug Deliv Rev 64:200–216. doi:10.1016/j.addr.2011.08.006
11. Saha K, Agasti SS, Kim C, Li X, Rotello VM (2012) Gold nanoparticles in chemical and biological sensing. Chem Rev 112:2739–2779. doi:10.1021/cr2001178
12. Jans H, Huo Q (2012) Gold nanoparticle-enabled biological and chemical detection and analysis. Chem Soc Rev 41:2849–2866. doi:10.1039/C1CS15280G
13. Liu X, Yu M, Kim H, Mameli M, Stellacci F (2012) Determination of monolayer-protected gold nanoparticle ligand–shell morphology using NMR. Nat Commun 3:1182. doi:10.1038/ncomms2155
14. Harkness KM, Balinski A, McLean JA, Cliffel DE (2011) Nanoscale phase segregation of mixed thiolates on gold nanoparticles. Angew Chem Int Ed 50:10554–10559. doi:10.1002/anie.201102882
15. Gentilini C, Pasquato L (2010) Morphology of mixed-monolayers protecting metal nanoparticles. J Mater Chem 20:1403–1412. doi:10.1039/b912759c
16. Carney RP, DeVries GA, Dubois C, Kim H, Kim JY, Singh C, Ghorai PK, Tracy JB, Stiles RL, Murray RW, Glotzer SC, Stellacci F (2008) Size limitations for the formation of ordered striped nanoparticles. J Am Chem Soc 130:798–799. doi:10.1021/ja077383m
17. Centrone A, Hu Y, Jackson AM, Zerbi G, Stellacci F (2007) Phase separation on mixed-monolayer-protected metal nanoparticles: a study by infrared spectroscopy and scanning tunneling microscopy. Small 3:814–817. doi:10.1002/smll.200600736
18. Jackson AM, Hu Y, Silva PJ, Stellacci F (2006) From homoligand- to mixed-ligand-monolayer-protected metal nanoparticles: a scanning tunneling microscopy investigation. J Am Chem Soc 128: 11135–11149. doi:10.1021/ja061545h
19. Jans K, Bonroy K, Palma RD, Reekmans G, Jans H, Laureyn W, Smet M, Borghs G, Maes G (2008) Stability of mixed PEO-thiol SAMs for biosensing applications. Langmuir 24:3949–3954. doi:10.1021/la703718t
20. Mantzila AG, Maipa V, Prodromidis MI (2008) Development of a faradic impedimetric immunosensor for the detection of *Salmonella typhimurium* in milk. Anal Chem 80:1169–1175. doi:10.1021/ac071570l
21. Mirmohseni A, Hosseini J, Shojaei M, Davaran S (2013) Design and evaluation of mixed self-assembled monolayers for a potential use in everolimus eluting coronary stents. Colloids Surf B 112:330–336. doi:10.1016/j.colsurfb.2013.07.069
22. Loaiza OA, Lamas-Ardisana PJ, Jubete E, Ochoteco E, Loinaz I, Cabanero G, García I, Penades S (2011) Nanostructured disposable impedimetric sensors as tools for specific biomolecular interactions: sensitive recognition of concanavalin A. Anal Chem 83:2987–2995
23. Hederos M, Konradsson P, Liedberg B (2005) Synthesis and self-assembly of galactose-terminated alkanethiols and their ability to resist proteins. Langmuir 21:2971–2980. doi:10.1021/la047203b
24. Li L, Chen S, Zheng J, Ratner BD, Jiang S (2005) Protein adsorption on oligo(ethylene glycol)-terminated alkanethiolate self-assembled monolayers: the molecular basis for nonfouling behavior. J Phys Chem B 109:2934–2941. doi:10.1021/jp0473321
25. Khoshtariya DE, Dolidze TD, Shushanyan M, Eldik RV (2014) Long-range electron transfer with myoglobin immobilized at Au/mixed-SAM junctions: mechanistic impact of the strong protein confinement. J Phys Chem B 118:692–706. doi:10.1021/jp4101569
26. Vasumathi V, Natalia M, Cordeiro DS (2014) Molecular dynamics study of mixed alkanethiols covering a gold surface at three different arrangements. Chem Phys Lett 600:79–86. doi:10.1016/j.cplett.2014.03.064
27. Hung S, Hwang J, Tseng F, Chang J, Chen C, Chieng C (2006) Molecular dynamics simulation of the enhancement of cobra cardiotoxin and E6 protein binding on mixed self-assembled monolayer molecules. Nanotechnology 17:S8–S13. doi:10.1088/0957-4484/17/4/002
28. Zheng J, Li L, Chen S, Jiang S (2004) Molecular simulation study of water interactions with oligo (ethylene glycol)-terminated alkanethiol self-assembled monolayers. Langmuir 20:8931–8938. doi:10.1021/la036345n
29. Hung S, Hsiao P, Lu M, Chieng C (2012) Thermodynamic investigations using molecular dynamics simulations with potential of mean force calculations for cardiotoxin protein adsorption on mixed self-assembled monolayers. J Phys Chem B 116:12661–12668. doi:10.1021/jp304695w
30. Ghorai PK, Glotzer SC (2010) Atomistic simulation study of striped phase separation in mixed-ligand self-assembled monolayer coated nanoparticles. J Phys Chem C 114:19182–19187. doi:10.1021/jp105013k
31. Lehn RCV, Alexander-Katz A (2013) Structure of mixed-monolayer-protected nanoparticles in aqueous salt solution from atomistic molecular dynamics simulations. J Phys Chem C 117: 20104–20115. doi:10.1021/jp406035e
32. Huang K, Ma H, Liu J, Huo S, Kumar A, Wei T, Zhang X, Jin S, Gan Y, Wang PC, He S, Zhang X, Liang X (2012) Size-dependent localization and penetration of ultrasmall gold nanoparticles in cancer cells, multicellular spheroids, and tumors in vivo. ACS Nano 6: 4483–4493. doi:10.1021/nn301282m
33. Kumar A, Ma H, Zhang X, Huang K, Jin S, Liu J, Wei T, Cao W, Zou G, Liang X (2012) Gold nanoparticles functionalized with therapeutic and targeted peptides for cancer treatment. Biomaterials 33:1180–1189. doi:10.1016/j.biomaterials.2011.10.058
34. Huo S, Jin S, Ma X, Xue X, Yang K, Kumar A, Wang PC, Zhang J, Hu Z, Liang X (2014) Ultrasmall gold nanoparticles as carriers for nucleus-based gene therapy due to size-dependent nuclear entry. ACS Nano 8:5852–5862. doi:10.1021/nn5008572
35. Trudel S (2011) Unexpected magnetism in gold nanostructures: making gold even more attractive. Gold Bull 44:3–13. doi:10.1007/s13404-010-0002-5
36. Lian S, Hu D, Zeng C, Zhang P, Liu S, Cai L (2012) Highly luminescent near-infrared-emitting gold nanoclusters with further natural etching: photoluminescence and $Hg^{2+}$ detection. Nanoscale Res Lett 7:348. doi:10.1186/1556-276X-7-348
37. Quinn BM, Liljeroth P, Ruiz V, Laaksonen T, Kontturi K (2003) Electrochemical resolution of 15 oxidation states for monolayer protected gold nanoparticles. J Am Chem Soc 125:6644–6645. doi:10.1021/ja0349305
38. Zhang T, Zhao H, He S, Liu K, Liu H, Yin Y, Gao C (2014) Unconventional route to encapsulated ultrasmall gold nanoparticles for high-temperature catalysis. ACS Nano 8:7297–7304. doi:10.1021/nn502349k
39. Lio A, Charych DH, Salmeron M (1997) Comparative atomic force microscopy study of the chain length dependence of frictional properties of alkanethiols on gold and alkylsilanes on mica. J Phys Chem B 101:3800–3805
40. Chang Y, Ukiwe C, Kwok DY (2005) Chain length effect of alkanethiol self-assembled monolayers on the maximum spreading ratio of impacting water droplets. Colloids Surf A 260:255–263. doi:10.1016/j.colsurfa.2005.03.015
41. Martin JE, Wilcoxon JP, Odinek J, Provencio P (2000) Control of the interparticle spacing in gold nanoparticle superlattices. J Phys Chem B 104:9475–9486. doi:10.1021/jp001292t
42. Malinsky MD, Kelly KL, Schatz GC, Van Duyne RP (2001) Chain length dependence and sensing capabilities of the localized surface

plasmon resonance of silver nanoparticles chemically modified with alkanethiol self-assembled monolayers. J Am Chem Soc 123:1471–1482. doi:10.1021/ja003312a

43. Liu FM, Kollensperger PA, Green M, Cass AEG, Cohen LF (2006) A note on distance dependence in surface enhanced Raman spectroscopy. Chem Phys Lett 430:173–176. doi:10.1016/j.cplett.2006.08.091
44. Agrawal PM, Rice BM, Thompson DL (2002) Predicting trends in rate parameters for self-diffusion on FCC metal surfaces. Surf Sci 515:21–35. doi:10.1016/S0039-6028(02)01916-7
45. Rai B, Sathis P, Malhotra CP, Pratip AKG (2004) Molecular dynamics simulations of self-assembled alkylthiolate monolayers on Au(111) surface. Langmuir 30:3138–3144. doi:10.1021/la0357256
46. Brooks BR, Bruccoleri RE, Olafson BD, States DJ, Swaminathan S, Karplus M (1983) CHARMM: a program for macromolecular energy, minimization, and dynamics calculations. J Comput Chem 4:187–217. doi:10.1002/jcc.540040211
47. Devi JM (2014) Aggregation of thiol coated gold nanoparticles: a simulation study on the effect of polymer coverage density and solvent. Comp Mater Sci 86:174–179. doi:10.1016/j.commatsci.2014.01.042
48. Lee O, Schatz GC (2009) Molecular dynamics simulation of DNA-functionalized gold nanoparticles. J Phys Chem C 113:2316–2321. doi:10.1021/jp8094165
49. Kalia RK, Nakano A, Vashishta P (2012) Supercrystals of DNA-functionalized gold nanoparticles: a million-atom molecular dynamics simulation study. J Phys Chem C 116:19579–19585. doi:10.1021/jp306133v
50. Phillips JC, Braun R, Wang W, Gumbart J, Tajkhorshid E, Villa E, Chipot C, Skeel RD, Kale L, Schulten K (2005) Scalable molecular dynamics with NAMD. J Comput Chem 26:1781–1802. doi:10.1002/jcc.20289
51. Jorgensen WL, Chandrasekhar J, Madura JD, Impey RW, Klein ML (1983) Comparison of simple potential functions for simulating liquid water. J Chem Phys 79:926–935. doi:10.1063/1.445869
52. Wiencek KM, Fletcher M (1995) Bacterial adhesion to hydroxyl- and methyl-terminated alkanethiol self-assembled monolayers. J Bacteriol 177:1959–1966
53. Callow ME, Callow JA, Ista LK, Coleman SE, Nolasco AC, Lopez GP (2000) Use of self-assembled monolayers of different wettabilities to study surface selection and primary adhesion processes of green algal (*Enteromorpha*) zoospores. Appl Environ Microbiol 66:3249–3254. doi:10.1128/AEM.66.8.3249-3254.2000
54. Li Y, Yang Z, Hu N, Zhou R, Chen X (2013) Insights into hydrogen bond dynamics at the interface of the charged monolayer-protected Au nanoparticle from molecular dynamics simulation. J Chem Phys 138:184703. doi:10.1063/1.4803504
55. Chen X, Hua W, Huang Z, Allen HC (2010) Interfacial water structure associated with phospholipid membranes studied by phase-sensitive vibrational sum frequency generation spectroscopy. J Am Chem Soc 132:11336–11342. doi:10.1021/ja1048237
56. Scatena LF, Brown MG, Richmond GL (2001) Water at hydrophobic surfaces: weak hydrogen bonding and strong orientation effects. Science 292:908–912. doi:10.1126/science.1059514
57. Heikkilä E, Gurtovenko AA, Martinez-Seara H, Häkkinen H, Vattulainen I, Akola J (2012) Atomistic simulations of functional $Au_{144}(SR)_{60}$ gold nanoparticles in aqueous environment. J Phys Chem C 116:9805–9815. doi:10.1021/jp301094m
58. Li J, Liu T, Li X, Ye L, Chen H, Fang H, Wu Z, Zhou R (2005) Hydration and dewetting near graphite−$CH_3$ and graphite−COOH plates. J Phys Chem B 109:13639–13648. doi:10.1021/jp044090w
59. Hua L, Huang X, Zhou R, Berne BJ (2006) Dynamics of water confined in the interdomain region of a multidomain protein. J Phys Chem B 10:3704–3711. doi:10.1021/jp055399y
60. Pal SK, Peon J, Bagchi B, Zewail AH (2002) Biological water: femtosecond dynamics of macromolecular hydration. J Phys Chem B 106:12376–12395. doi:10.1021/jp0213506
61. Yoo H, Paranji R, Pollack GH (2011) Impact of hydrophilic surfaces on interfacial water dynamics probed with NMR spectroscopy. J Phys Chem Lett 2:532–536. doi:10.1021/jz200057g
62. He Y, Chang Y, Hower JC, Zheng J, Chen S, Jiang S (2008) Origin of repulsive force and structure/dynamics of interfacial water in OEG–protein interactions: a molecular simulation study. Phys Chem Chem Phys 10:5539–5544. doi:10.1039/B807129B
63. Russo D, Hura G, Head-Gordon T (2004) Hydration dynamics near a model protein surface. Biophys J 86:1852–1862. doi:10.1016/S0006-3495(04)74252-6